

Seismic Performance of Simple Reinforced Masonry Houses with Brick Walls: Experimental and Numerical Approaches

Namira Risza Pasya, Ashar Saputra, Angga Fajar Setiawan, Henricus Priyosulistyo

Department of Civil Engineering, University of Gadjah Mada, Yogyakarta, INDONESIA

E-mail: saputra@ugm.ac.id

| Submitted: March 04, 2025 | Revised: September 30, 2025 | Accepted: December 19, 2025 |

| Published: December 31, 2025 |

ABSTRACT

This study aims to evaluate the performance of brick houses against earthquakes through experimental and numerical approaches. The research objects include two single-story houses located at University of Gadjah Mada (UGM) and Turi, Sleman, Yogyakarta. Microtremor measurement was carried out using accelerometers to record building vibrations, which were then analyzed using Fast Fourier Transform (FFT) to obtain the natural frequency on site of the structure. Numerical modeling was carried out using finite element analysis to validate and assess the building's frequency response to earthquake loads based on Service Level Earthquake (SLE), Design Basis Earthquake (DBE), and Maximum Considered Earthquake (MCE). The results of the study indicate that the modeling can be validated based on the natural frequency approach from field and numerical evaluate. The maximum displacement that occurred at the SLE, DBE, and MCE levels exceeded the allowable limits, indicating that both houses are in an unsafe condition. The structural performance evaluation based on Federal Emergency Management Agency (FEMA 356) shows that the houses in UGM and Turi fall into the Collapse Prevention (CP) category, which mean that the building can no longer be used as houses on the verge of collapse. Although the maximum acceleration analysis of the houses indicates that the values are lower than the design peak ground acceleration (PGAm), structural failure may still occur. The results of this study are expected to provide insights into earthquake-resistant house design as well as recommendations for improving structural resistance to seismic load.

Keywords: accelerometers, FFT, performance evaluation, residential houses, structural vulnerability.

INTRODUCTION

Earthquakes are highly destructive disasters that can cause structural damage to buildings, especially for houses that use brick as a building material. The earthquake incident that occurred in Yogyakarta in 2006 recorded significant damage to 175.671 houses, showing the importance of research on the performance of single-story houses with brick materials during an earthquake [14]. This incident emphasizes the urgency of conducting a structural performance evaluation to ensure the safety of the building's occupants.

Studies have shown that vibration amplification can occur in certain parts of a building, such as the ring beam and ground floor. Factors that affect this amplification include earthquake frequency, building material properties, and structural configuration [7]. To analyze the structural response to earthquakes, the response spectrum method is applied since it provides an overview of the dynamic behavior of a building to various levels. This method considers important parameters such as the natural vibration period of the building and earthquake characteristics, thus it can be used to evaluate the deviations that occur due to earthquake loads at various levels of severity [10].

Vibration measurement using accelerometers is an effective method to obtain data on building response to earthquakes because it provides the information of frequency and amplitude accurately [15]. The data obtained are analyzed using the FFT technique to identify the dynamic characteristics of the building in more detail. The results of this analysis are then used in numerical modeling using ETABS software, which allows simulation of building behavior against various earthquake load scenarios [8]. In addition, building performance is evaluated based on targets that have been established in [5], including performance categories such as Immediate Occupancy (IO), Life Safety

(LS), and Collapse Prevention (CP) [12]. Several previous studies have stated that brick houses are highly vulnerable to earthquake loads due to the brittle nature of the material and the lack of structural reinforcement [2].

This study aims to evaluate the performance of residential buildings by measuring the natural frequency of the structure through field testing and conducting numerical modeling using the finite element method. This approach is expected to provide insights into the safety level of houses against dynamic loads, particularly those caused by earthquakes. The performance of residential buildings against lateral loads generated by earthquakes is greatly influenced by the elastic modulus of the material, the dimensions of the structure, and the reinforcement system used. Therefore, an in-depth analysis regarding the behavior of residential structures against earthquakes is crucial by considering these various parameters.

METHOD

Research Location

The research location was chosen based on the similarity of building characteristics: a one-story house with brick walls and a relatively similar building area. This allows for a precise comparison of the influence of certain factors on structural performance. The research was conducted in two locations as seen in Figure 1, which are University of Gadjah Mada as House A (in red) and Turi as House B (in green), Sleman Regency, Yogyakarta. The distance between the houses is 19.4 km.



a. Yogyakarta's location on the Central Java map
(source: Google)

b. Location of the two houses
(source: Google Maps)

Figure 1. Location of the measured houses on the Central Java map (a) and distance between House A (in red) and House B (in green) (b)

Measurement

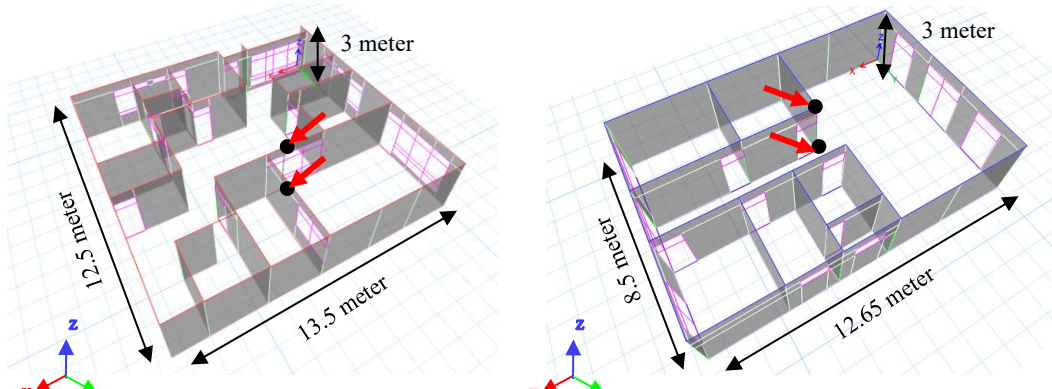
The measurements were conducted on House A and House B using a PCB accelerometer with a sensitivity of 1000mV/g and installed on the ring beam and ground floor to record the vibration response of the building. This position contributes to the stiffness and stability of the building. The ring beam can detect lateral deformation and global behavior of the structure, while the ground floor reflects the overall movement of the structure against the ground. The existing condition of the houses and the specifications of the sensor positions for both houses can be seen in Figure 2 and Figure 3. The data obtained include the acceleration and natural frequency of the building for 5 minutes, which are then analyzed to identify the dynamic characteristics of the building structure [9]. The frequency used is the average of the frequencies observed at the ring beam and the base. Vibration recordings were conducted in two principal directions to analyze the dynamic response of the building structure to earthquake loads. The X direction is defined as the longitudinal direction of the building, which is parallel to the longest side of the structure, while the Y direction is the transverse direction, perpendicular to the X direction. Before the measurements began, the accelerometer was calibrated to ensure a zero reading when the instrument was motionless.



a. Existing condition of House A

b. Existing condition of House B

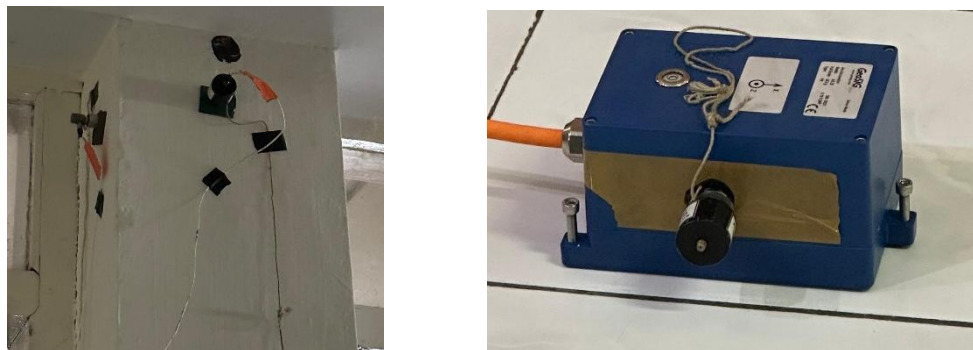
Figure 2. Existing condition of House A (a) and House B (b)



a. Position of the sensor at House A

b. Position of the sensor at House B

Figure 3. The position of the sensors in House A (a) and House B (b)



a. Position of the sensor on the ring beam

b. Position of the sensor on the base

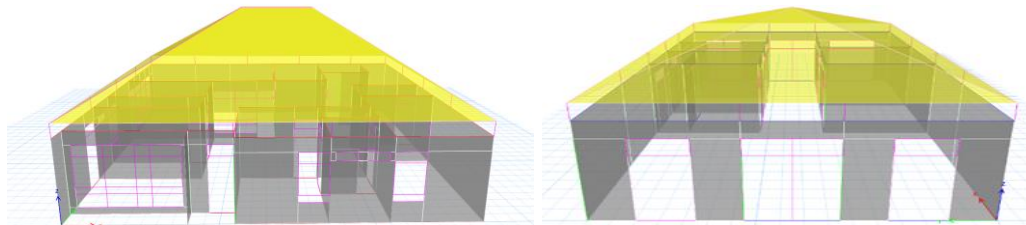
Figure 4. The position of the sensors on the ring beam (a) and base (b)

Numerical Modeling

Numerical modeling using Finite Element Method (FEM) was carried out based on the accurate data of the houses in the field, including dimensions and material characteristics (see Table 1). The structure was modeled using a finite element approach, where the masonry walls were represented by shell elements (see Figure 5). Both houses used masonry materials with a concrete quality of 20 MPa [6] and an elastic modulus of 1500 MPa [11].

Table 1. Dimensions of the material used

Location	Column cm	Block cm	Tie Column cm	Casement cm
UGM	30 x 15 and 30 x 30	15 x 30	15 x 15	8 x 12
Turi	30 x 15	15 x 30 and 20 x 15	15 x 15	8 x 12



a. Structural modeling of House A

b. Structural modeling of House B

Figure 5. Structural modeling of both measured houses

Dead loads and live loads are considered as the self-weight of the structure in accordance with the provisions of [3]. The earthquake load used was obtained from the website <https://rsa.ciptakarya.pu.go.id/2021/>, which provides a design response spectrum based on SNI 1726:2019. The earthquake parameters (see Table 2) and the analysis was conducted using the spectrum response method.

Table 2. Seismic data at both house locations

Location	S _s g	S ₁ g	T _L second	PGA g
UGM	1.1300	0.5072	6	0.4873
Turi	0.9301	0.4382	20	0.4002

Both measured houses have the same earthquake load parameters in accordance with the provisions of SNI 1726:2019. These buildings are classified as Risk Category II, indicating that these residential houses fall into the category of buildings with a moderate risk of earthquake impact. The seismic importance factor (I_e) used is 1.0, which aligns with the standard for residential buildings that do not require an increased reliability factor against earthquake load.

The building structure adopts a seismic force-resisting system in the form of an ordinary moment-resisting reinforced concrete frame, which has limited deformation capacity in resisting lateral forces caused by earthquakes. Additionally, an upper-limit coefficient of the fundamental period (C_u) value of 1.4 is used to limit the estimated fundamental vibration period of the building in seismic analysis. Both houses have a building height of 3 meters, which is consistent with the typical standard for single-story houses. These parameters serve as the basis for evaluating the structural response to earthquakes to ensure the safety and performance of the buildings under various levels of earthquake intensity.

The load combinations used include dead load (D), live load (L), vertical earthquake load (E_v) = $0.2S_{DS}D$, and horizontal earthquake load (E_h) = ρQ_E , in accordance with SNI 1726:2019 article 4.2.2. The reduction factors and load factors applied are in accordance with the provisions to ensure the safety of the structure. This load combination is modeled in ETABS, where load cases are automatically calculated in the structural analysis. The load combination is calculated based on Table 3.

Table 3. Load combination for the ultimate limit state (ULS) method

Load Combination	Dead	Live	Vertical Earthquake	Horizontal Earthquake
	D	L	E_v	E_h
1.4D	1.4			
1.2D + 1.6L	1.2	1.6		
1.2D + E_v + E_h + L	1.2	1	± 0.9	± 1.3
0.9D - E_v + E_h	0.9		± 0.9	± 1.3

Research Flow

The vibration recording data was processed using DewesoftX including a filtering process to reduce noise, before being analyzed using FFT to determine the natural frequencies of the building. The results were visualized in a frequency spectrum graph. Validation was carried out by comparing the results of field tests with numerical modeling, which includes natural frequencies. Furthermore, structural performance analysis was carried out on three earthquake variants, namely Service Level Earthquake (SLE), Design Basis Earthquake (DBE), and Maximum Considered Earthquake (MCE) based on FEMA 356 guidelines to evaluate the seismic capacity and performance of the building. Maximum ground acceleration (PGA_M) was calculated based on SNI 1726:2019, considering site factors and floor acceleration as the basis for evaluating the resistance of structures to earthquake loads. The research flow diagram can be seen in Figure 9.

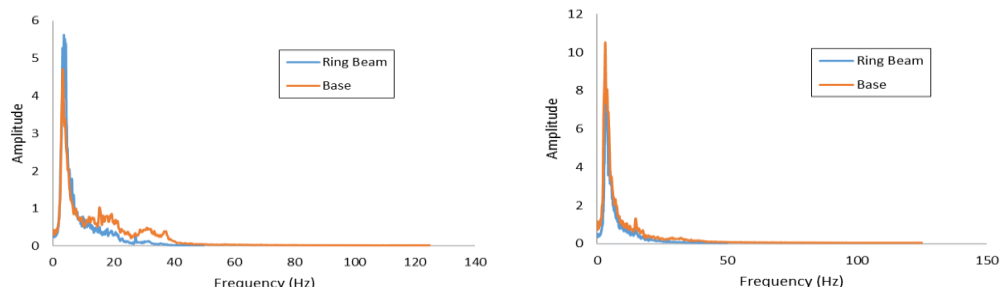
RESULTS AND DISCUSSION

The natural frequency of the building

The natural frequencies of the buildings were obtained through field testing using accelerometers and numerical modeling. The analysis results show an acceptable agreement between the natural frequencies obtained from both methods, with the differences between the results of field measurements and numerical simulations (see Table 4). Graphic average frequency longitudinal and transverse can be seen Figure 6 and Figure 7. These differences can be caused by several factors, including model idealization, assumptions of placement conditions that may differ from actual conditions, and uncertainties in material parameters such as elastic modulus and structural mass. Nevertheless, the results of this comparison indicate that numerical modeling is able to represent the dynamic characteristics of the building with an acceptable level of accuracy, hence it can be used as a valid analysis tool to evaluate structural responses to dynamic loads.

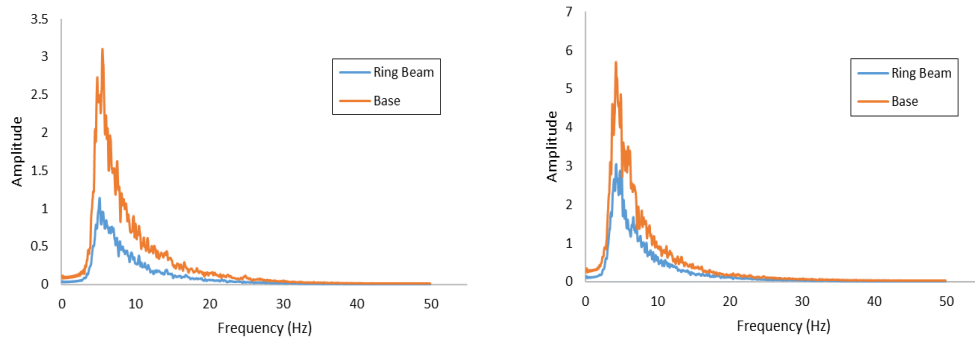
Table 4. Comparison of natural frequencies between test and numerical

Direction	UGM		Difference		Turi		Difference	
	In field (Hz)	Numerical (Hz)	%	In field (Hz)	Numerical (Hz)	%		
Longitudinal	3.420	3.626	5.7	5.374	5.109	4.9		
Transverse	3.237	3.398	4.7	4.226	3.977	5.9		



(a) Longitudinal dominant frequency graph (b) Transverse dominant frequency graph.

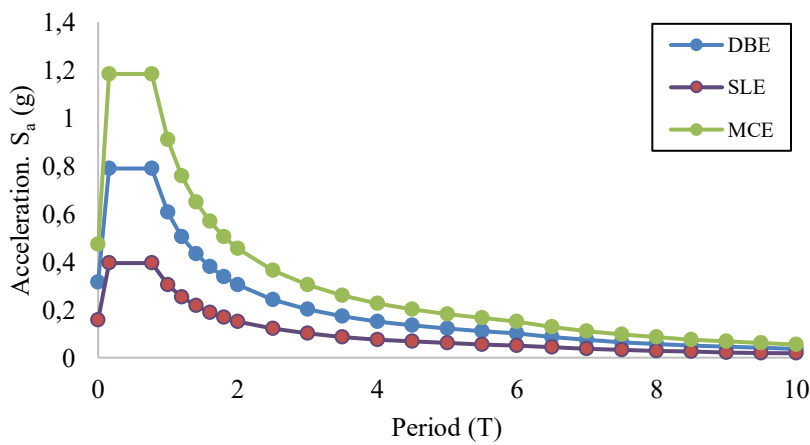
Figure 6. Longitudinal (a) and Transverse (b) dominant frequency graphic at House A



(a) Longitudinal dominant frequency graph (b) Transverse dominant frequency graph.

Figure 7. Dominant frequency graphic at House B**Spectrum Response**

The evaluation of building performance against earthquake loads is carried out by considering three levels of earthquake occurrence: Service Level Earthquake (SLE), Design Basis Earthquake (DBE), and Maximum Considered Earthquake (MCE). SLE represents an earthquake with a high probability of occurrence but low intensity, DBE is used as the basis for designing structures during their service life, while MCE describes the largest possible earthquake scenario with a minor probability. In the numerical analysis, each earthquake variation is modeled using the spectrum response method based on SNI 1726:2019 (see Figure 8 and Figure 10). This spectrum response data is derived through the S_{MS} multiplier coefficient (short-period spectrum acceleration) and S_{MI} (1-second spectrum acceleration), which depend on the seismic parameters of the test location. The application of this analysis aims to evaluate the capacity of the structure to withstand earthquake loads according to different levels of intensity. The results of the analysis are used to determine whether the building has performance that meets safety standards and whether reinforcement is needed to increase its resistance to severe earthquake scenarios.

**Figure 8.** Combined response spectrum of earthquake variations at House A

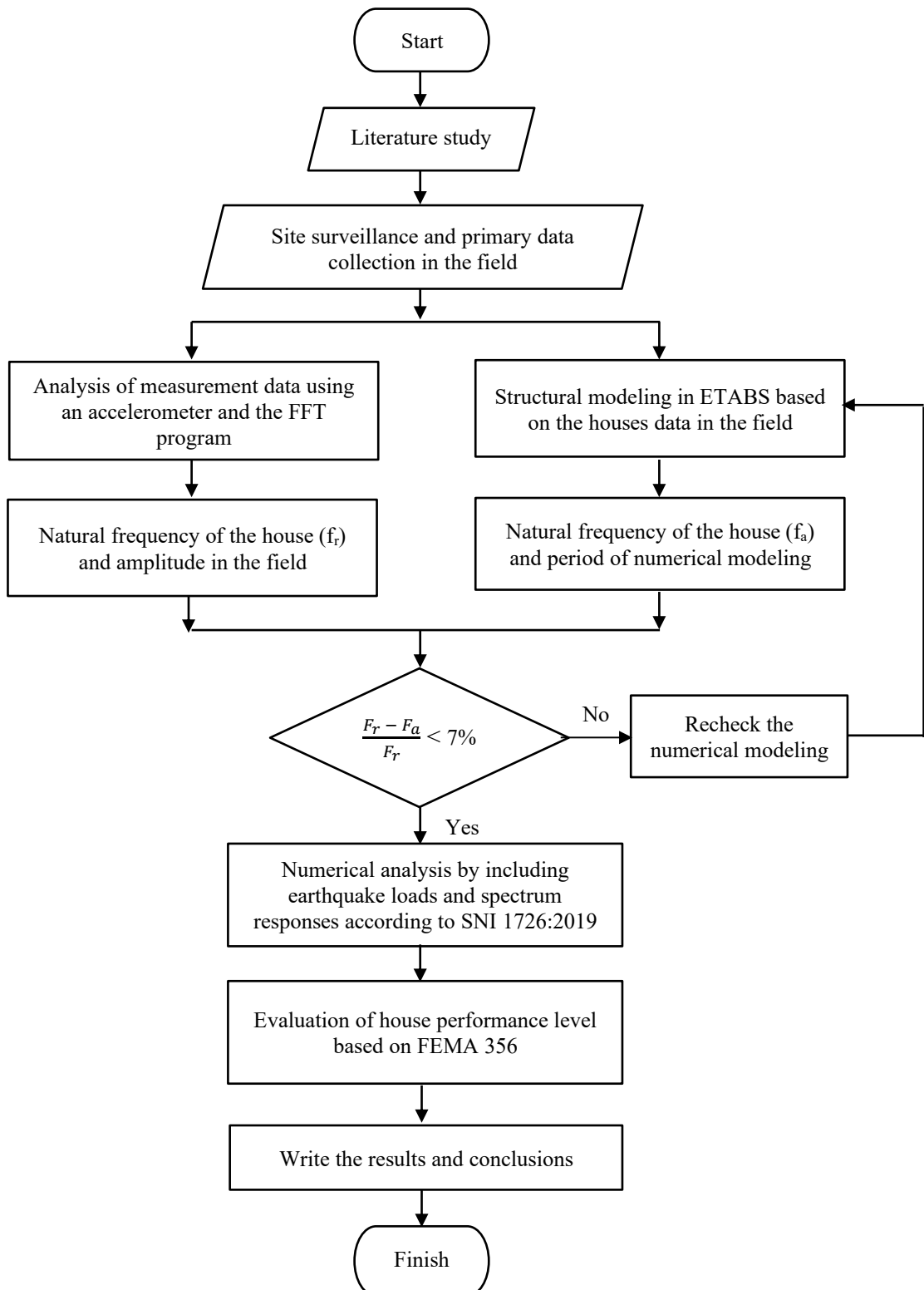


Figure 9. Research flowchart

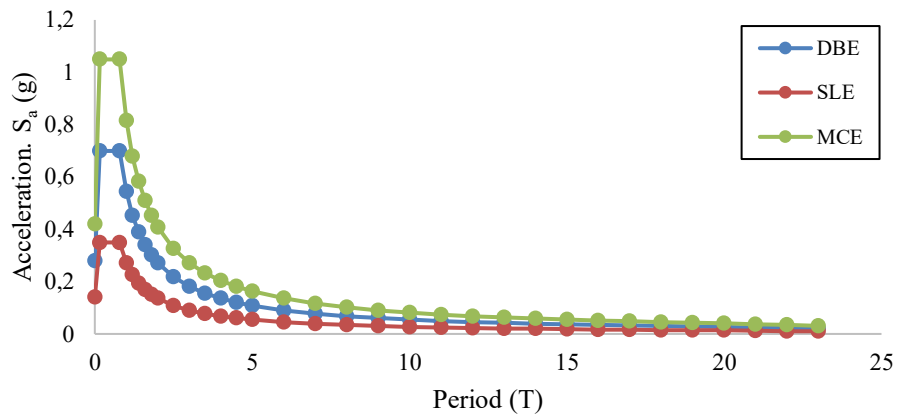


Figure 10. Combined response spectrum of earthquake variations at House B
Structural Displacement

The inelastic drift of House A (UGM) and House B (Turi) exceeds the drift limit, indicating that the buildings are in an unsafe condition. The allowable inelastic lateral drift for reinforced masonry, as derived from NTC-M, is 0.0025 times the building height [1]. The largest displacement in House A and House B occurred during the MCE earthquake variation which has an earthquake recurrence period of 2475 years. The largest displacements in House A, based on Table 7, were 24.023 mm in the X (longitudinal) direction and 39.220 mm in the Y (transverse) direction. Meanwhile, in House B, the largest displacements in the X (longitudinal) and Y (transverse) directions were recorded respectively at 11.500 mm and 18.373 mm (see Table 10). Based on Tables 5 to 10, the maximum drift values for both houses exceed the allowable drift limits in both the longitudinal and transverse directions. This indicates that the buildings exhibit poor seismic performance and are at risk of structural failure under the three analyzed variations of earthquake loads. A comparison of the displacement between House A and House B shows that House A is more vulnerable to structural failure than House B. One of the influencing factors is the age of House A, which has reached 33 years, thus affecting the building's characteristics.

Table 5. Displacement at the SLE level of House A

Story	Displacement		Elastic Drift		h	Inelastic Drift		Drift Limit	Check
	δe_x	δe_y	δe_x	δe_y		Δ_x	Δ_y		
	(mm)	(mm)	(mm)	(mm)		(mm)	(mm)	(mm)	
Ringbeam	4.384	7.333	4.384	7.333	3000	10.960	18.333	7.50	Not ok
Base	0	0	0	0	0	0	0	0	

Table 6. Displacement at the DBE level of House A

Story	Displacement		Elastic Drift		h	Inelastic Drift		Drift Limit	Check
	δe_x	δe_y	δe_x	δe_y		Δ_x	Δ_y		
	(mm)	(mm)	(mm)	(mm)		(mm)	(mm)	(mm)	
Ringbeam	6.792	11.219	6.792	11.219	3000	16.980	28.048	7.50	Not ok
Base	0	0	0	0	0	0	0	0	

Table 7. Displacement at the MCE level of House A

Story	Displacement		Elastic Drift		h	Inelastic Drift		Drift Limit	Check
	δe_x	δe_y	δe_x	δe_y		Δ_x	Δ_y		
	(mm)	(mm)	(mm)	(mm)		(mm)	(mm)	(mm)	
Ringbeam	9.609	15.688	9.609	15.688	3000	24.023	39.220	7.50	Not ok
Base	0	0	0	0	0	0	0	0	

Table 8. Displacement at the SLE level of House B

Story	Displacement		Elastic Drift		h	Inelastic Drift		Drift Limit	Check
	δe_x (mm)	δe_y (mm)	δe_x (mm)	δe_y (mm)		Δ_x (mm)	Δ_y (mm)		
Ringbeam	2.162	3.562	2.162	3.562	3000	5.405	8.905	7.50	Not ok
Base	0	0	0	0	0	0	0	0	

Table 9. Displacement at the DBE level of House B

Story	Displacement		Elastic Drift		h	Inelastic Drift		Drift Limit	Check
	δe_x (mm)	δe_y (mm)	δe_x (mm)	δe_y (mm)		Δ_x (mm)	Δ_y (mm)		
Ringbeam	3.483	5.616	3.483	5.616	3000	8.708	14.040	7.50	Not ok
Base	0	0	0	0	0	0	0	0	

Table 10. Displacement at the MCE level of House B

Story	Displacement		Elastic Drift		h	Inelastic Drift		Drift Limit	Check
	δe_x (mm)	δe_y (mm)	δe_x (mm)	δe_y (mm)		Δ_x (mm)	Δ_y (mm)		
Ringbeam	4.600	7.349	4.600	7.349	3000	11.500	18.373	7.50	Not ok
Base	0	0	0	0	0	0	0	0	

Building Performance Evaluation

The building performance level can be evaluated based on the drift ratio parameters, namely the building risk category and earthquake variations according to the FEMA 356 regulations. The performance evaluation of both houses can be seen in Table 11 and Table 12. The analysis results indicate that House A has a higher potential for earlier collapse than House B. It's proven by the fact that in the SLE earthquake variation, House A has reached the Collapse Prevention (CP) category, meaning that the building is at risk of total failure due to severe structural damage and extreme deformation, rendering it unusable. Meanwhile, House B falls into the Life Safety (LS) category, indicating that the building has sustained significant structural and non-structural damage but remains standing with minimal risk to human life. At the MCE earthquake level, both houses suffered severe damage, rendering them uninhabitable, with indications that they had reached the CP category. The following is the performance evaluation of both houses.

Table 11. Building performance evaluation in House A

Earthquake Variation	X Direction	Y Direction	Performance Level
SLE	0.37%	0.61%	LS – CP
DBE	0.57%	0.93%	LS – CP
MCE	0.80%	1.31%	CP – CP

Table 12. Building performance evaluation in House B

Earthquake Variation	X Direction	Y Direction	Performance Level
SLE	0.18%	0.30%	IO – LS
DBE	0.29%	0.47%	LS – LS
MCE	0.38%	0.61%	LS – CP

Maximum Acceleration

Building safety can be evaluated by comparing nodal acceleration to the design peak ground acceleration. Based on [4], the design ground acceleration is used as a reference for earthquake-resistant building design. A one-story house has a lower acceleration than a multi-story building. The smaller the acceleration, the more elastic a building is and is able to absorb the effects of earthquakes well. If the acceleration exceeds the design value, the risk of building damage increases.

Therefore, structural planning must consider the effects of acceleration to ensure optimal seismic resilience [13].

Table 13. Safety evaluation of House A, MCE earthquake case

Direction	Nodal	Nodal	Design Peak Ground	Safety Level
	Acceleration mm/sec ²	Acceleration Gal	Acceleration Gal	
Longitudinal	3782.42	378.242	531.917	Safe
Transverse	5292.52	529.252	531.917	Safe

Table 14. Safety evaluation of House B, MCE earthquake case

Direction	Nodal	Nodal	Design Peak Ground	Safety Level
	Acceleration mm/sec ²	Acceleration Gal	Acceleration Gal	
Longitudinal	3671.89	367.189	471.037	Safe
Transverse	3596.34	359.634	471.037	Safe

Table 13 and 14 above means that both houses are at a safe level because the nodal acceleration is lower than the PGA_M . This suggests that the dynamic response of the structure to seismic loads remains within acceptable limits, thereby minimizing the risk of damage due to seismic acceleration. Additionally, the difference in nodal acceleration values between the longitudinal and transverse directions reflects the dynamic characteristics of the structure, which are influenced by the stiffness and mass of the building.

CONCLUSION

The natural frequencies obtained from testing in House A (UGM) and House B (Turi) differ by less than 7% compared to numerical modeling, indicating that the modeling accurately represents the actual characteristics of the buildings in the field. The measurement results indicate that the displacement that occurring in House A and House B due to various earthquake variations (SLE, DBE, and MCE) exceeds the allowable displacement limits, meaning that the buildings are in an unsafe condition and at risk of collapse. The structural failure of both houses can be assessed based on the building performance evaluation guidelines in FEMA 356. House A, the structural performance of the SLE and DBE earthquake variations is categorized as Life Safety (LS) in the X direction and Collapse Prevention (CP) in the Y direction. While for the MCE earthquake variation, it's in the CP category in both directions (X and Y). Meanwhile, House B indicated the Immediate Occupancy (IO) and Life Safety (LS) categories in the X and Y directions for SLE earthquake variations. Structural performance of the DBE earthquake variation, House B reaches the LS category in both directions (X and Y). In the MCE earthquake variation, the house remains in the LS category for the X direction but falls into the CP category for the Y direction.

In addition to displacement evaluation, both houses were also analyzed in terms of the observed the maximum acceleration and the design Peak Ground Acceleration (PGA_M). The maximum acceleration in House A was recorded at 141.841 Gal in the longitudinal direction and 198.470 Gal in the transverse direction, while the PGA_M reached 531.917 Gal. Meanwhile, House B, the maximum acceleration was recorded at 137.696 Gal in the longitudinal direction and 134.863 Gal in the transverse direction, with a PGA_M of 471.037 Gal.

Although the maximum acceleration that occurred was lower than the PGA_M , the displacement evaluation results indicate that both houses have exceeded the acceptable displacement limits and have entered the CP category, indicating the potential for total structural failure. This condition may be caused by several factors, such as structural design that does not meet performance standards and the potential degradation or lower material quality than initially designed. Therefore, further monitoring and strengthening strategies are required to ensure the sustainability of structural performance and mitigate the risk of failure in the future.

REFERENCES

- [1]. Alcocer, S. M., Cesin, J., Flores, L. E., Hernandez, O., Meli, R., Tena, A., and Vasconcelos, D. (2003). The New Mexico City Building Code Requirements for Design and Construction of Masonry Structures. North American Masonry Conference.
- [2]. Alidoust, P., Keramati, M., Hamidian, P., Amlashi, A. T., Gharehveran, M. M., & Behnood, A. (2021). Prediction of the shear modulus of municipal solid waste (MSW): An application of machine learning techniques. *Journal of Cleaner Production*, 303, 127053.
- [3]. Badan Standardisasi Nasional. (2019). SNI 1726:2019 Tata Cara Perencanaan Ketahanan Gempa Untuk Struktur Bangunan Gedung dan Nongedung. Jakarta.
- [4]. European Committee for Standardization (CEN). (2004). Eurocode 8: Design of structures for earthquake resistance – Part 1: General rules, seismic actions and rules for buildings (EN 1998-1:2004). Brussels, Belgium: CEN.
- [5]. Federal Emergency Management Agency. (2000). FEMA 356: Pre standard and Commentary for the Seismic Rehabilitation of Buildings. Washington, DC.
- [6]. Hendry, E., (2001). Masonry Walls: Materials and Construction. *Construction and Building Materials* 15 (2001) 323-330. [https://doi.org/10.1016/S0950-0618\(01\)00019-8](https://doi.org/10.1016/S0950-0618(01)00019-8).
- [7]. Jalayer, F., Der Kiureghian, A., and Lee, C. (2009). Seismic Performance Evaluation of Structures Using Performance-Based Seismic Design Methodology. *Journal of Structural Engineering*, 135(12) 1733-1745.
- [8]. Kurniawan, A. S. P. B. (2020). Review Kekuatan Gedung Terhadap Gempa Bumi (Membandingkan Uji Eksperimen dan Numerik Gedung Lab Bahan Bangunan UGM). Universitas Gadjah Mada. Yogyakarta.
- [9]. Li, F., Xie, Z., Zhang, L., Yu, X., & Shi, B. (2025). Intelligent long-term prediction of wind-induced response of super high-rise buildings during typhoons based on wind tunnel tests. *Journal of Building Engineering*, 112144.
- [10]. Nugroho, F. A., Nurchasanah, Y., and Fauzi, M. G. (2024). Evaluasi Kinerja Struktur Gedung Menggunakan Analisis Respons Spektrum Gempa Desain SNI 1726:2019. Universitas Muhammadiyah Surakarta.
- [11]. Paulay and Priestley. (1992). Seismic Design of Reinforced Concrete and Masonry Buildings. A Wiley Interscience Publication. United States of America.
- [12]. Pribadi, P. A. (2022). Evaluasi Kinerja Struktural Gedung Fasilitas Pendidikan Asrama Mahasiswa 3 Lantai Bentuk Persegi Panjang Dengan Gempa Kala Ulang 475 Tahun Berdasarkan ASCE 41-17. Universitas Gadjah Mada. Yogyakarta.
- [13]. Seed, H. B., & Idriss, I. M. (1971). Simplified Procedure for Evaluating Soil Liquefaction Potential. *Journal of Soil Mechanics and Foundations Div., ASCE*.
- [14]. Widodo, A. (2024). Belajar dari Gempa Jogja 27 Mei 2006. Institusi Teknologi Sepuluh Nopember. Surabaya.
- [15]. Zhao, Z., Chen, Z., and Zhang, L. (2011). Application of Accelerometer-Based Dynamic Testing for Structural Health Monitoring. *Journal of Vibration and Acoustics*, 133(5), 051004.